Mössbauer study of neutron-irradiated Fe-Ni-Cr-Mo-Si-B metallic glass

Marcel Miglierini*
Department of Material Physics, Faculty of Engineering Science, Osaka University, Toyonaka, Osaka 560, Japan
(Received 22 April 1991)

Effects of neutron irradiation on $Fe_{30}Ni_{48-x}Cr_xMo_2Si_5B_{15}$ glassy ribbons are studied by transmission ^{57}Fe Mössbauer spectroscopy. The spectra are fitted using NORMOS DIST programs accounting for line asymmetries. Bimodal $P(H)$ distributions are obtained, and they are presented in the form of three-dimensional graphs, the second dimension in these projections being built from Cr content and neutron fluence, respectively. A neutron-irradiation-induced ferromagnetic-to-paramagnetic transition is observed. Changes in the hyperfine parameters are supposed to be governed by a rearrangement of the constituent atoms, including clustering of Cr and by stress centers because of irradiation.

I. INTRODUCTION

Irradiation of metallic glasses leads to structural modifications which are reflected through changes of various magnetic parameters such as Curie temperature,[1,2] orientation of the net magnetic moment,[3,4] and hyperfine field distributions.[5] Chromium-containing metallic glasses show advantageous properties for practical purposes mainly because of their high corrosion resistance. That is why they are the subject of intense research in many laboratories.[6–9] Because of possible applications under extreme conditions of increased radiation (nuclear facilities, cosmic research, etc.), their response to different kinds of radiation damage should be known.

The aim of the present work is to study the influence of neutron irradiation or amorphous $Fe_{30}Ni_{48-x}Cr_xMo_2Si_5B_{15}$. It was reported by Violet *et al.* [10] that, regarding Fe-Ni-Zr metallic glasses, the effects of neutron irradiation on the magnetic properties of these alloys are small, suggesting rather a good resistance to neutron radiation damage up to fluences of 10^{17} n/cm^2. Kramer, Johnson, and Cline[11] revealed a significant influence of neutron irradiation ranging from 10^{18} to 10^{20} n/cm^2 on superconducting $(Mo_{0.6}Ru_{0.4})_{82}B_{18}$ metallic glass. We have chosen neutron fluences from 10^{14} to 10^{19} n/cm^2, and this allows one to observe the effects of irradiation in a wide range. Using ^{57}Fe Mössbauer spectroscopy, our interest is focused on changes in magnetic parameters comprising the direction of the net magnetic moment with respect to the glass ribbon surface, the average value, and the standard deviation of the distributions of hyperfine parameters, including both the distributions of the hyperfine fields, $P(H)$, and the distributions of the quadrupole splittings, $P(u)$.

Mössbauer spectroscopy is an useful tool, especially when information about the nearest surroundings of the resonant atoms is needed. Changes in their configuration are sensitively reflected through the parameters of the Mössbauer spectra, and hence conclusions concerning the influence of neutron irradiation on amorphous $Fe_{30}Ni_{48-x}Cr_xMo_2Si_5B_{15}$ are made.

II. EXPERIMENT

$Fe_{30}Ni_{48-x}Cr_xMo_2Si_5B_{15}$ metallic glass was prepared in the form of 6-mm-wide and 16–27-μm-thick ribbons by the melt-spinning technique at the Institute of Physics, Slovak Academy of Sciences, Bratislava. Samples with chromium content x of 0, 2, 4, 6, 8, 10, and 12 at. % were sealed in Al foils and exposed to the whole neutron spectrum in a nuclear research reactor. Integrated fluences were in the range from 10^{14} to 10^{19} n/cm^2. The temperature of the samples during irradiation was maintained under 70 °C.

A conventional constant-acceleration Mössbauer spectrometer with a $^{57}Co(Rh)$ source was used in transmission geometry. The spectra were recorded at room temperature using α-Fe calibration. They were fitted by the NORMOS DIST program developed by Brand.[12] A simple histogram method (DISTRI = 1) using 30 sextets and 16 doublets was applied to obtain distributions of hyperfine magnetic fields, $P(H)$, and quadrupole splittings, $P(u)$, respectively. A linewidth of 0.30 mm/s was assumed for all individual subspectra. Spectrum asymmetries were covered by fitting the parameters related to a linear change in isomer shift values (ISO and DTI in METHOD=2, respectively 6) and to a short-range order (SRO) (I_p, H_{1p}, Q_p, and H_{2p}) for magnetically split patterns. The area ratio D_{23} of lines 2 and 5 to lines 3 and 4 in the Mössbauer spectra showing ferromagnetic ordering was also fitted during the analysis. The only exception was the spectrum of the sample with 8 at. % of Cr, where $D_{23}=2$ was fixed while evaluating its very poorly resolved sextet. The area ratio D_{13} of lines 1,6 to 3,4 was constrained to have a constant value of 3 in all cases.

III. RESULTS AND DISCUSSION

A. Mössbauer spectra

Room-temperature Mössbauer spectra of amorphous $Fe_{30}Ni_{48-x}Cr_xMo_2Si_5B_{15}$ taken in the as-received state and after neutron irradiation with a fluence of 10^{19} n/cm^2 are shown in Figs. 1(a) and 1(b), respectively. As can be

seen from these figures, their shape is changing, while the Cr content x in the samples varies. Continuous, x-dependent transformation of the primary six line patterns into doublets implies a reduction of ferromagnetic exchange interaction, giving rise to a total magnetic long-range-order collapse into pure paramagnetic behavior. A compositional-dependent decrease of the Curie temperature T_c is revealed, and it is associated with changes in the chemical SRO.[6,7,13–15] The actual values of T_c for the present sample, derived from temperature dependences of the initial permeability, have already been reported.[16] The observed shapes of the Mössbauer spectra, including central doublets, indicate that there exists a distribution of hyperfine fields with a noticeable population at the low-field side.[8,9] The influence of varying the amount of Cr on the magnetic ordering of nonirradiated amorphous $Fe_{30}Ni_{48-x}Cr_xMo_2Si_5B_{15}$ is discussed elsewhere[17,18] in more detail comprising low-temperature Mössbauer experiments. Here we will take a closer look into changes in the magnetic structure introduced by neutron irradiation.

During neutron irradiation, defects are generated in metallic glasses. Topological SRO is mainly affected by[1,19] (i) displacements of atoms caused by high-energy α (1.4 MeV) and Li (0.9 MeV) particles which are created in boron-containing metallic glasses in accordance with the nuclear reaction $^{10}B(n,\alpha)^7Li+2.3$ MeV and (ii) displacements of atoms caused by fast neutrons. Some modifications of the composition can also be expected because, especially when higher fluences are used, the α particles agglomerate and form helium bubbles.[3,20] On the other hand, irradiation-induced changes in the elements presented in the samples were evaluated to be negligible.[19]

As can be seen from Fig. 1(a), the ferromagnetic-to-paramagnetic transition occurs beyond $x=8$ as the amount of Cr in the as-received samples increases. When the specimens were irradiated with a fluence of 10^{19} n/cm^2, the transition to the paramagnetic state appeared at a smaller x value. Figure 1(b) shows that this critical Cr content at room temperature is $x=6$. This suggests a decrease in T_c because of neutron irradiation. Such an effect was observed and reported previously[16]. However, the decrease of T_c because of neutron irradiation is not a general feature of Cr-doped metallic glasses. It depends on the amount of Fe and Cr in the sample whether the T_c value will be increased, decreased, or even not changed at all, as we will discuss later in this paper.

To illustrate the effects of neutron irradiation on the Mössbauer spectra more closely, we have chosen some of

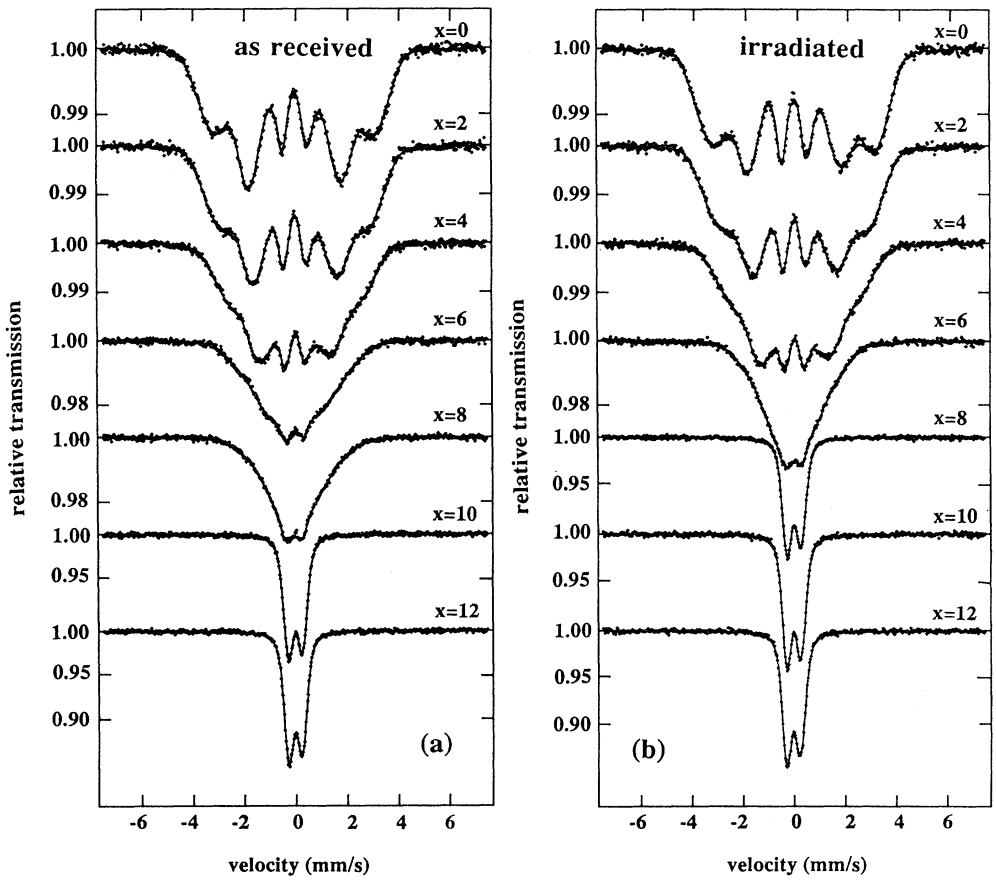

FIG. 1. Room-temperature Mössbauer spectra of $Fe_{30}Ni_{48-x}Cr_xMo_2Si_5B_{15}$ metallic glass (a) before and (b) after neutron irradiation with 10^{19} n/cm^2.

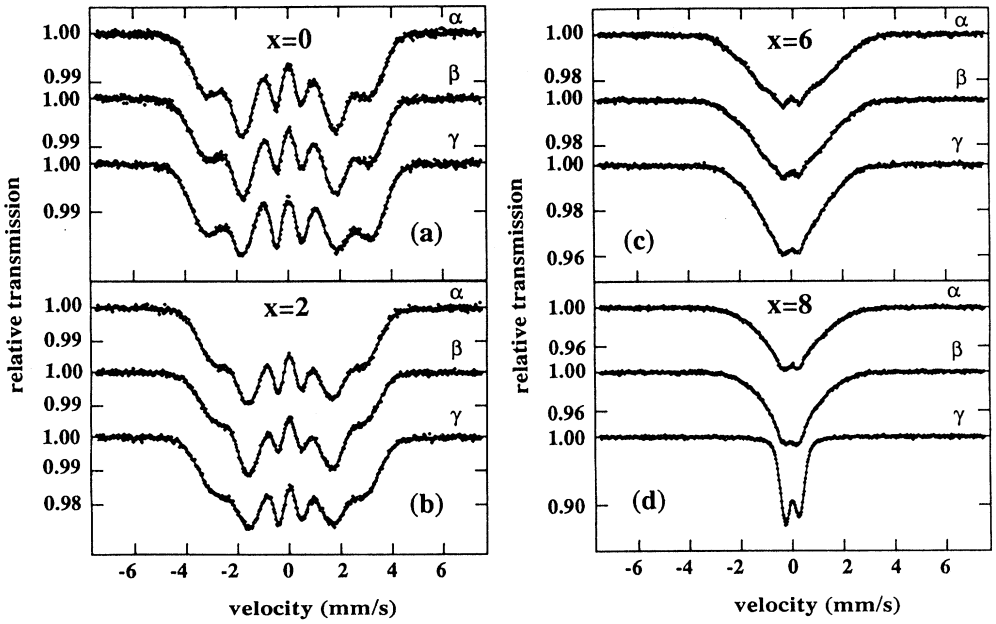

FIG. 2. Room-temperature Mössbauer spectra of $Fe_{30}Ni_{48-x}Cr_xMo_2Si_5B_{15}$ metallic glass for the indicated Cr contents x. Spectra labeled as α, β, and γ correspond to the as-received sample and to the samples irradiated with 10^{18} and 10^{19} n/cm^2, respectively.

the most typical examples, which are displayed in Fig. 2. Going from the uppermost to the lowermost spectrum in each part of the figure, the spectra are labeled as α, β, and γ for the as-received sample and samples irradiated with a fluence of 10^{18} n/cm^2 and with $\Phi=10^{19}$ n/cm^2, correspondingly. Qualitative changes in the shapes of the Mössbauer spectra after neutron irradiation are depicted in Figs. 2(c) and 2(d). As can be seen from Fig. 2(c), the spectrum of the $x=6$ sample is gradually "narrowed," while the fluence is rising. This means that ferromagnetic exchange interactions are continuously reduced and paramagnetic ordering prevails. Finally, a complete irradiation-induced ferromagnetic-to-paramagnetic transition is shown in Fig. 2(d) ($x=8$ at. % Cr). It occurred after exposing the sample with a neutron fluence of 10^{19} n/cm^2. The change in magnetic ordering is demonstrated by the qualitative distinctions between the β and γ spectra when, in the case of the γ, only a pure quadrupole doublet is seen.

B. Net magnetic moments

Looking at Figs. 2(a) and 2(b) where the respective Mössbauer spectra for $x=0$ and 2 are depicted, one can notice, by comparing the β and γ curves, a decrease of the second and fifth line intensities (areas) after neutron irradiation with a fluence of 10^{19} n/cm^2. The fitting parameter D_{23} gives the ratio between the intensities (areas) of lines 2,5 and 3,4. Since D_{23} is related to a relative orientation between γ rays and a net magnetic moment of an absorber, an average direction of the net magnetic moment can be determined with respect to the plane of the sample.

The fluence dependences of the differences in the area ratios, ΔD_{23}, for magnetically split Mössbauer spectra are seen in Fig. 3. Here ΔD_{23} represents changes of D_{23} after neutron irradiation in comparison with the as-received state: $\Delta D_{23}=D_{23_{\text{irradiated}}}-D_{23_{\text{as-received}}}$. The majority of the measured spectra consists of very poorly resolved sextets, and that is why we present the differences ΔD_{23} rather than the D_{23} values themselves, the accuracy of which may be questioned. Data for $x=8$ are not shown. In this case only a small amount of a ferromagnetic component is presented in the sample, as is evident from the corresponding Mössbauer spectra in Fig. 2(d). To evaluate such spectra, D_{23} had to be fixed ($D_{23}=2$) during the fitting procedure. The dashed lines in Fig. 3 cover deviations within the experimental error.

Negative ΔD_{23} values imply that the net magnetic moment is turned out from its original position and comes to be more perpendicularlike. For $x=0$ such behavior can be observed along with the rising neutron fluence. The final direction of the moment deviated after irradiation with 10^{19} n/cm^2 of about 10° from its close-to-the-ribbon plane position in the as-received state. The same tendency of the net magnetic moment to turn out of the ribbon plane was reported for Fe-Ni-B–type metallic glasses both after irradiation with heavy ions[3,4] and with neutrons,[5] and depending on the magnetostriction of the samples, this behavior was also observed regarding some Cr-doped metallic glasses.[2,4,21] On the other hand, positive ΔD_{23} values suggest a rotation of the net magnetic moment toward the plane of the sample. A fluence-dependent tendency of the net magnetic moment to turn closer to the ribbon plane for $x=4$ at. % of Cr is revealed from an increase of ΔD_{23} in Fig. 3. The observed changes in the direction of the net magnetic moment, reflected through the line intensities, are supposed to be a

consequence of a reorientation of spins in the vicinity of stress centers, which are generated as a result of atom mixing after neutron irradiation.[2-5,21]

The domain structure of rapidly quenched alloys is governed by microstructural defects and their stress fields.[22] Kuzmann and Spirov[4] reported a decrease of the second and fifth Mössbauer line intensities of $Fe_{40}Ni_{40}B_{10}Si_{10}$ metallic glass to be due to the defects induced by irradiation which are responsible for the reorientation of spins. The above results suggested that the SRO and distribution of magnetic dipoles are affected by in-plane compressive stresses in the irradiated regions. Serfözö *et al.*[2] found that in the case of $Fe_{78-x}Cr_xSi_8B_{14}$ these stresses induce an easy magnetization direction normal to the surface of the sample through positive magnetostriction. Our recent results on $Fe_{80}Cr_2Si_4B_{14}$ metallic glass[21] are fully consistent with their findings and in the present case, this behavior is well established for $x=0$ (Fig. 3).

Although transmission (bulk) Mössbauer experiments revealed no crystalline phases in the irradiated samples, a contribution of partially crystallized surface layers to the above-discussed effects cannot be unambiguously ruled out.[3,23-25] Surface crystallization causes a compressive stress in the bulk of the specimen acting in the ribbon plane because of the higher density of the crystalline phase with respect to the amorphous one. In specimens with a positive magnetostriction, this compressive stress would tend to rotate the atomic spins in a direction out of the ribbon plan and vice versa.[23] Using both conversion electron Mössbauer spectroscopy (CEMS) and scanning electron microscopy, Nasu and Fujita[24] reported the presence of α-Fe at both sides of amorphous Fe-B-Si ribbon which was irradiated by 25-kV accelerated He^+ ions. They also observed a decrease of the Mössbauer line intensities because of the increase of total bombardment flux, suggesting that the orientation of magnetic moments became more random. Hayashi *et al.*[25] revealed a precipitation of crystalline α-Fe in the near-surface regions when they irradiated amorphous Fe-B alloys with 40-keV He^+ ions. The amorphous-to-crystalline transformation has been reported to be dependent on the irradiation fluence. To identify the presence of crystalline regions, they used a depth-selective conversion electron Mössbauer spectroscopy (DCEMS). However, as stated by Gupta *et al.*[23], conclusions about a surface crystallization can be made also from changes in the direction of the net magnetic moment which are reflected through bulk Mössbauer spectrum line intensities.

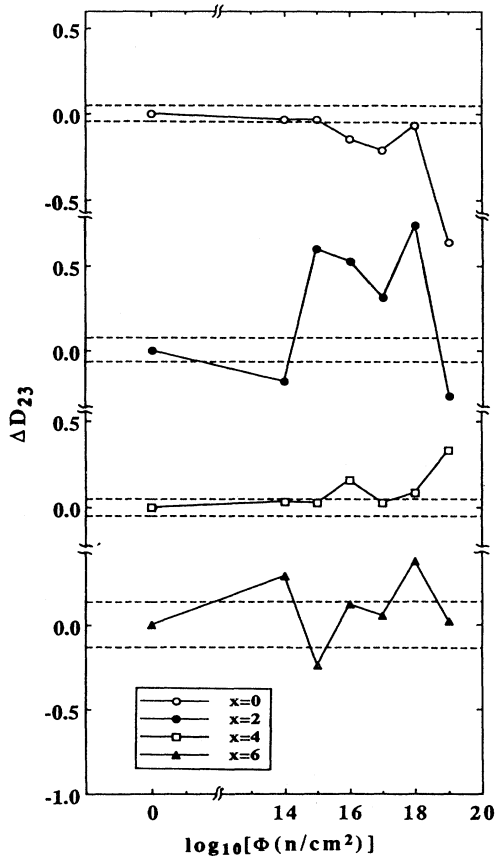

FIG. 3. Differences ΔD_{23} (see text) plotted vs logarithm of neutron fluence, $\log_{10}\Phi$, for amorphous $Fe_{30}Ni_{48-x}Cr_xMo_2Si_5B_{15}$. The solid lines are only guides to the eye. The dashed lines cover deviation within the experimental error.

C. Quadrupole splitting distributions

As far as the Mössbauer spectra for both as-received and irradiated samples with $x=10$ and 12 at. % Cr are concerned, all of them are asymmetric doublets in shape showing distributions of quadrupole splittings, $P(u)$. The same behavior is observed for the sample with $x=8$ at. % of Cr irradiated by $\Phi=10^{19}$ n/cm^2. Examples of $P(u)$ distributions for $x=12$ before and after irradiation with 10^{19} n/cm^2 are shown in Fig. 4. It is noteworthy that the zero $2u$ values have nonzero probabilities. This feature was also observed in $Cr_{72-x}Fe_xC_{17}Si_8Al_3$ metallic glasses.[26] Mean values of the $P(u)$ distributions, $\langle 2u \rangle$, and the isomer shifts, δ (relative to α-Fe), are plotted against the logarithm of a neutron fluence $\log_{10}\Phi$ and shown in Figs. 5(a) and 5(b), respectively. There was no

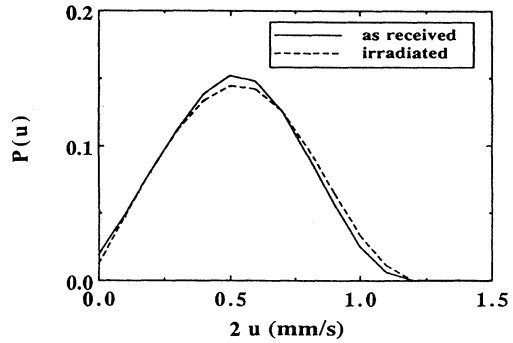

FIG. 4. Quadrupole splitting distributions $P(u)$ for amorphous $Fe_{30}Ni_{48-x}Cr_xMo_2Si_5B_{15}$ before and after neutron irradiation with 10^{19} n/cm^2.

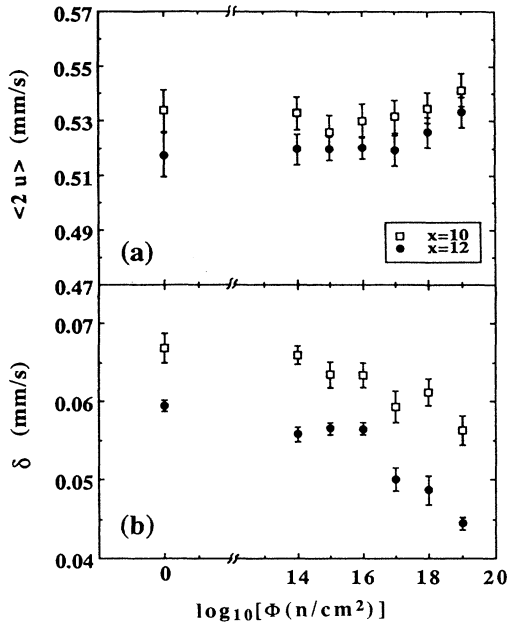

FIG. 5. (a) Average value of a quadrupole splitting distribution $\langle 2u \rangle$ and (b) isomer shift δ (relative to α-Fe) vs logarithm of neutron fluence, $\log_{10}\Phi$, for amorphous $Fe_{30}Ni_{48-x}Cr_2Mo_2Si_5B_{15}$.

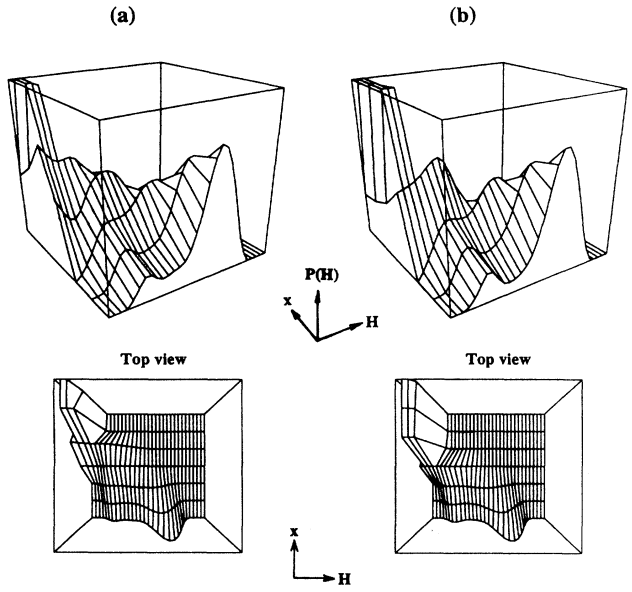

FIG. 6. 3D $P(H)$ distributions corresponding to the room-temperature Mössbauer spectra of amorphous $Fe_{30}Ni_{48-x}Cr_xMo_2Si_5B_{15}$ (see Fig. 1) (a) before and (b) after irradiation with 10^{19} n/cm^2. The second dimension is built from the Cr content x. See the text for details.

change in the standard deviation of the $P(u)$ distributions within the experimental error.

The observed changes in $\langle 2u \rangle$ and δ suggest that Fe atoms have different environments and occupy different positions after irradiation. This irradiation effect surely occurs because a decrease of the Curie temperature after neutron irradiation was revealed for the $x=12$ sample both from low-temperature Mössbauer experiments and from the temperature dependence of the ac magnetic susceptibility[27] and T_c was shown to be very sensitive to atomic structure rearrangement processes in Cr-containing Fe-Ni–based amorphous alloys.[28,29]

D. Hyperfine field distributions

The observed shapes of the Mössbauer spectra in Fig. 1 suggest that there is a broad distribution of hyperfine fields with a noticeable population at the low-field side. To derive the distributions $P(H)$, the measured spectra were fitted by a simple histogram method accounting also for the spectrum asymmetries.

Similar as in Ref. 18, we present three-dimensional (3-D) graphs of the obtained $P(H)$ distributions. They were created by stacking the corresponding distributions according to either Cr content x or the logarithm of the neutron fluence, $\log_{10}\Phi$. Figure 6 presents 3D $P(H)$ distributions. The second dimension was built from x, before and after irradiation with a fluence of 10^{19} n/cm^2. These distributions correspond to the Mössbauer spectra from Figs. 1(a) and 1(b), respectively.

The bimodal character of the individual distributions can be recognized. It arises from the presence of a central doublet in addition to a ferromagnetic sextet pointing out mixed hyperfine interactions at $T<T_c$.[30] This unusual two-peak sturture of $P(H)$ is a point of controversy in the literature (see, for example, Refs. 31 and 32), but evidently small hyperfine fields do exist (again, Refs. 31 and 32), even though their origin is not completely understood.[30,33] It is reasonable to assume that the low-field component in $P(H)$ should be associated with those Fe atoms that are surrounded by a considerable amount of neighboring Cr atoms, whereas the high-field one is due to those Fe atoms that have primarily Fe and Ni atoms as their neighbors and, possibly, some Cr atoms sitting next to them.[14,34] The bimodal character of the $P(H)$ distributions corresponding to the sample with $x=0$ at. % of Cr is then due to molybdenum, which is in the same column of the periodic table as Cr and affects the magnetic properties similarly.[35–37]

Regarding the as-received samples, behavior of the $P(H)$ distributions along the rising Cr concentration is described elsewhere[17,18] in more detail. Here we will discuss the influence of neutron irradiation on the distribution of hyperfine fields. Before doing this, however, we must note that the distributions for $x=10$ and 12 and $x=8$, 10, and 12, which correspond to the Mössbauer spectra of the as-received and irradiated ($\Phi=10^{19}$ n/cm^2) samples, respectively, are in fact $P(u)$ distributions, as was already mentioned in Sec. III C.

In order to be able to show changes in the magnetic ordering more clearly using only a single figure, these $P(u)$ distributions have been converted to the H scale and drawn together with the $P(H)$ ones. They can be seen in the left-hand, rear corners ($H\rightarrow 0T$, $x\rightarrow 12$ at. % of Cr) of the 3D graphs in Fig. 6 creating sharp peaks. $P(W)$

values, where W represents H and $2u$, correspondingly, of all the distributions have been normalized to fulfill the condition $\int_{-\infty}^{\infty} P(W)dW=1$. That is why some of the $P(u)$ values were cut off in order to scale the whole figure properly.

As can be seen from Fig. 6(a), the bimodal character of the $P(H)$ distributions gradually vanishes with increasing Cr content, giving rise to a total ferromagnetic-to-paramagnetic transition between $x=8$ and 10. When irradiated with a fluence of 10^{19} n/cm^2 [see Fig. 6(b)], the onset of paramagnetism appears just at the concentration of 8 at. % of Cr. This change in magnetic ordering is also evident from the shapes of the corresponding Mössbauer spectra, which are depicted in Fig. 2(d) by the β and γ curves, and it will also be demonstrated by the fluence dependence of the hyperfine field distributions later in this section. The views from the top of the 3D graphs that are also shown in Fig. 6 show a more rapid shift of the high-field component toward smaller H values after neutron irradiation. Plots of the average values of the $P(H)$ distributions, $\langle H \rangle$, and their standard deviations, σ_H, against the Cr concentration x are shown in Fig. 7. It is noteworthy that after irradiation both these parameters are changed in a different direction with respect to their original values and to the amount of Cr in the samples. Since the σ_H values were calculated using the second moment of the $P(H)$ curves, their decrease suggests that the low-field component prevails, which, in turn, implies an increasing importance of quadrupole interactions near the magnetic ordering temperature. This can be supported by a completed transformation of the primary mixed hyperfine interactions into pure paramagnetic behavior in the case of $x=8$ after irradiation, and that is why no data related to this sample are presented in Fig. 7.

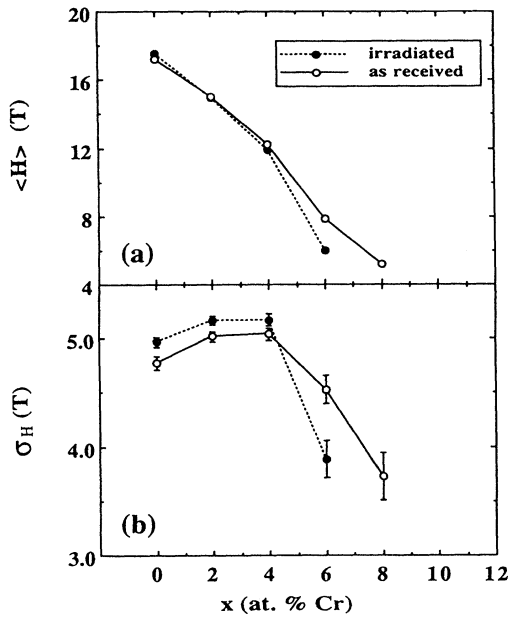

FIG. 7. (a) Average value of a hyperfine field distribution $\langle H \rangle$ and (b) standard deviation σ_H vs Cr content x for amorphous $Fe_{30}Ni_{48-x}Cr_xMo_2Si_5B_{15}$ before and after neutron irradiation with 10^{19} n/cm^2.

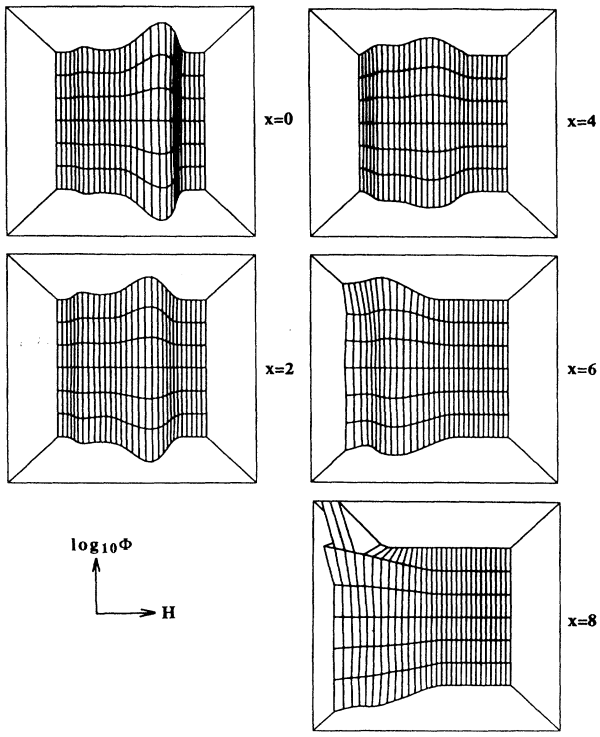

FIG. 8. Top views of the 3D $P(H)$ distributions corresponding to the room-temperature Mössbauer spectra of amorphous $Fe_{30}Ni_{48-x}Cr_xMo_2Si_5B_{15}$ for the indicated Cr contents x. The second dimension is built from the logarithm of neutron fluence, $\log_{10}\Phi$.

To demonstrate the changes of the $P(H)$ distributions induced by a varying neutron fluence for the respective concentration, the corresponding 3D projections are shown in Fig. 8. In this case the second dimension is represented by a logarithm of neutron fluence, $\log_{10}\Phi$. We have chosen views from the top which allowed us to observe directly the positions of the distribution peaks.

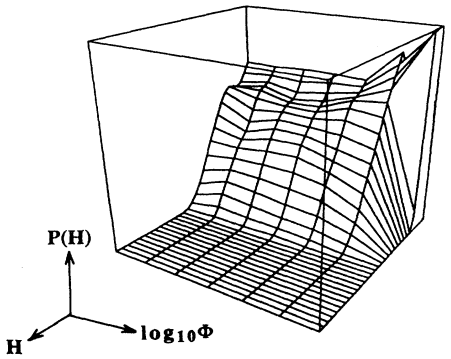

FIG. 9. 3D projection of the $P(H)$ distributions corresponding to the room-temperature Mössbauer spectra of amorphous $Fe_{30}Ni_{40}Cr_8Mo_2Si_5B_{15}$. The second dimension is built from the logarithm of neutron fluence, $\log_{10}\Phi$. See the text for details.

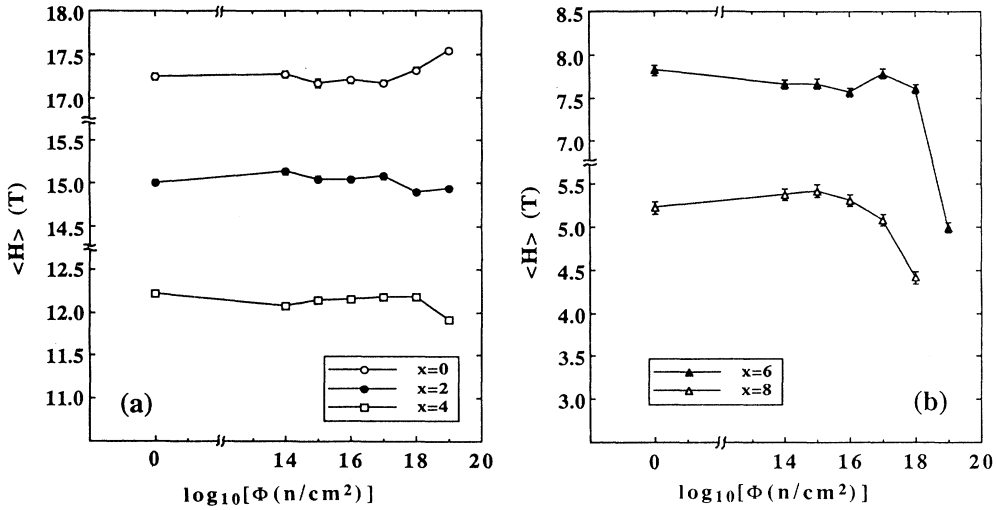

FIG. 10. Average value of a hyperfine field distribution $\langle H \rangle$ plotted vs logarithm of neutron fluence, $\log_{10}\Phi$, for the indicated Cr contents in amorphous $Fe_{30}Ni_{48-x}Cr_xMo_2Si_5B_{15}$. The solid lines are only guides to the eye.

As can be seen, for $x=0$ the peaks are more separated from one another after the irradiation, for $x=2$ their positions are nearly unchanged, and in the case of $x=4$, a slight shift of the peaks to the left is seen after irradiation with 10^{19} n/cm^2. Finally, a rapid shift toward low-field values is observed for $x=6$ and 8 after irradiation with $\Phi > 10^{17}$ n/cm^2. It should be mentioned that for $x=8$ the distribution corresponding to a fluence of 10^{19} n/cm^2 is a $P(u)$ distribution which has been converted to the H scale similary as in Fig. 6. The 3D graph of $x=8$ distributions is also depicted in Fig. 9 from another viewpoint to illustrate the irradiation-induced ferromagnetic-to-paramagnetic transition which occurs between applied fluences of 10^{18} and 10^{19} n/cm^2.

In Figs. 10 and 11 plots of $\langle H \rangle$ and σ_H, respectively, against the logarithm of neutron fluence, $\log_{10}\Phi$, are displayed. For $x=0$ a continuous increase of $\langle H \rangle$ values is observed along the neutron fluence. Practically no change is detected for $x=2$, and first of all a slight, then rather rapid decrease of $\langle H \rangle$ for $x=4$ and $x=6$ and 8, respectively, is revealed. The values of σ_H undergo both concentration- and fluence-dependent changes. The former are closely discussed in Ref. 18, while the latter show expected behavior only for $x=0$ and 4. The decrease of σ_H values in Fig. 11(b) suggests prevailing quadrupole interactions near the Curie temperature.

E. Radiation damage

To interpret the neutron-irradiation-induced changes of the parameters and $P(H)$ distributions investigated, the character of the processes of radiation damage must

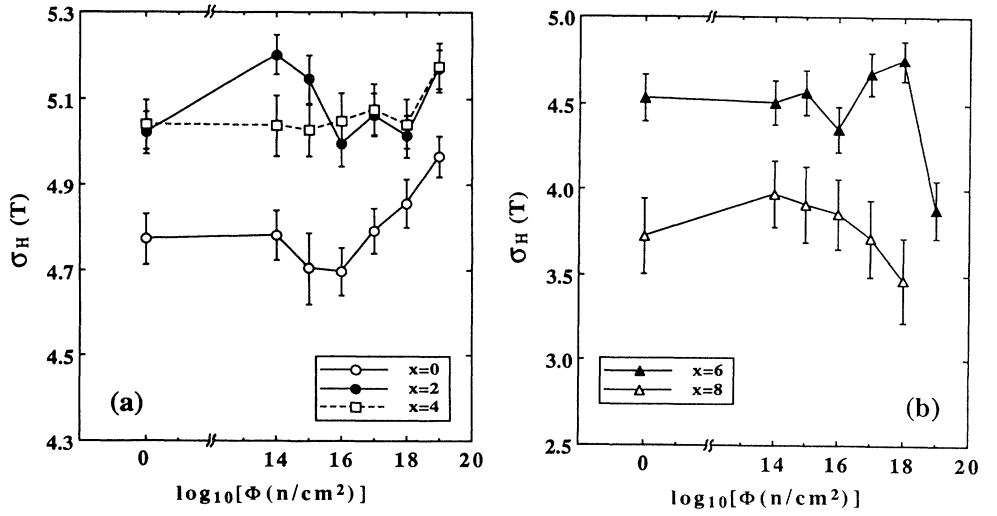

FIG. 11. Standard deviation of a hyperfine field distribution σ_H plotted vs logarithm of neutron fluence, $\log_{10}\Phi$, for the indicated Cr contents in amorphous $Fe_{30}Ni_{48-x}Cr_xMo_2Si_5B_{15}$. The solid and dashed lines are only guides to the eye.

be taken into consideration.

It was already mentioned in Sec. III A that the radiation damage comes from two sources, including high-energy particles and neutrons. The early stage of damage involves the creation of the primary knock on atoms when the irradiation particles transfer their energy to the lattice atoms and, in the next step, distribute this energy to the neighboring atoms and produce atomic displacements. The collision cascades created by recoiling target atoms contain highly disordered, high-temperature zones (10^2–10^3 K) (Ref. 38) which collapse or "cool down" at the estimated quench rate of 10^{14} or 10^{15} K/s. These processes lead to irradiation-induced structural changes by which the irradiated alloy disorders and usually loses its SRO.[11,38] This is demonstrated by an increase of the standard deviations of $P(H)$ distributions in Fig. 11. However, a rather rapid decrease of σ_H values is also seen in Fig. 11(b). It can be ascribed to changes in the character of $P(H)$ distributions when the low-field component comes to dominate.

Three-dimensional projections of $P(H)$ distributions presented in Figs. 6, 8, and 9 revealed changes in the peak positions, i.e., in the character of the corresponding distributions. Accounting for this, a clustering of Cr atoms after irradiation is proposed that causes the low-field part of the distributions to dominate, which, in turn, implies a reduction of ferromagnetic exchange interactions. These changes strongly depend on the amount of Cr in the sample.

IV. CONCLUSION

Summarizing the results of the Mössbauer study on neutron-irradiated $Fe_{30}Ni_{48-x}Cr_xMo_2Si_5B_{15}$ metallic glass in a wide fluence range, the following conclusions can be made.

(i) The shapes of Mössbauer spectra are sensitive to the influence of neutron irradiation, especially when fluences higher than 10^{17} n/cm^2 are used, enabling us to observe changes in magnetic ordering.

(ii) The direction of the net magnetic moment is controlled by both Cr concentration (magnetostriction of the sample) and rearrangement of the spins because of neutron irradiation. A contribution of surface crystallization to the observed effect is also possible.

(iii) Changes in the SRO were revealed, and they are reflected through the hyperfine field parameters, indicating clustering of Cr atoms. Cr atoms probably leave the high-field side of the $P(H)$ distribution, giving rise to the creation of additional Fe-Fe, Fe-Ni, and also Fe-Cr pairs. It is only a question of the relative amount of Fe, Ni, and Cr atoms in the sample what kind of exchange interaction comes to prevail. In the limit of high Cr content, an irradiation-induced ferromagnetic-to-paramagnetic transformation is seen. On the other hand, the same mechanism, i.e, the decrease of a number of Cr atoms in the high-magnetic-moment Fe sites, causes the low-field peak of $P(H)$ to move to the left and the high-field peak is shifted to the right when only a small amount of Cr is present in the sample, and a consequent increase of $\langle H \rangle$ values is observed. Regarding the present sample, this effect is clearly seen for $x=0$ at. % of Cr, and a tendency toward this behavior is revealed for $x=2$. The apparent controversy in the former case (no Cr in the sample) is overcome if we assume that Mo affects the magnetic properties of $Fe_{30}Ni_{48-x}Cr_xMo_2Si_5B_{15}$ metallic glass in the same way as Cr does.[35–37] We have also taken the results achieved from a Mössbauer study of neutron-irradiated $Fe_{80}Cr_2Si_4B_{14}$ (Ref. 21) into consideration.

(iv) Changes in the hyperfine field values suggest that the Curie temperature is affected by neutron irradiation.

ACKNOWLEDGMENTS

Discussions with Dr. I. Škorvánek in the early stage of this work are gratefully acknowledged. The amorphous samples were kindly provided by Dr. P. Duhaj. The author is indebted to Professor S. Nasu who made possible his stay at the Osaka University and to the Japanese Ministry of Education, Science and Culture (Monbuscho) for financial support. Thanks are also due to Professor S. Nasu for a critical reading of the manuscript and for valuable suggestions.

*On leave from the Department of Nuclear Physics and Technology, Slovak Technical University, Mlynská dolina, CS-812 19 Bratislava, Czechoslovakia.

[1]P. J. Grundy, G. A. Jones, and S. F. Parker, IEEE Trans. Magn. **MAG-19**, 1913 (1983).

[2]G. Serfözö, L. F. Kiss, Cs. S. Daróczi, E. Kisdi-Koszó, G. Vértesy, and A. Slawska-Waniewska, IEEE Trans. Magn. **MAG-16**, 1418 (1990).

[3]A. Bhagawat, M. B. Kurup, K. G. Prasad, and R. P. Sharma, Hyperfine Interact. **29**, 1167 (1986).

[4]E. Kuzmann and I. N. Spirov, Hyperfine Interact. **29**, 1175 (1986).

[5]M. Miglierini, J. Sitek, S. Balúch, J. Cirák, and J. Lipka, Hyperfine Interact. **55**, 1037 (1990).

[6]P. Auric, J. M. Greneche, O. deBouvier, and J. J. Rameau, J. Magn. Magn. Mater. **82**, 234 (1989).

[7]G. Serfözö, E. Kisdi-Koszó, A. Slawska-Waniewska, L. Potocký, S. Joneliunas, and M. Baran, Phys. Status Solidi A **118**, 307 (1990).

[8]W. Dudek, J. Gwiazda, E. Marianska, J. Oleniacz, and W. Zych, J. Magn. Magn. Mater. **86**, 213 (1990).

[9]S. Prasad, V. Srinivas, S. N. Shringi, A. K. Nigam, G. Chandra, and R. Krishnan, J. Magn. Magn. Mater. **92**, 92 (1990).

[10]C. E. Violet, R. J. Borg, L. May, K. V. Rao, J. Nogues, R. D. Taylor, and A. P. Batra, Hyperfine Interact. **42**, 963 (1988).

[11]E. A. Kramer, W. L. Johnson, and C. Cline, Appl. Phys. Lett. **35**, 815 (1979).

[12]R. A. Brand, NORMOS programs, internal report, Angewandte Physik, Universität Duisburg, 1987 (unpublished).

[13]K. Inomata, M. Hasegawa, and S. Shimanuki, IEEE Trans. Magn. **MAG-17**, 3076 (1981).

[14]S. T. Lin, L. Y. Jang, and D. P. Chiang, J. Phys. F. **17**, 1231 (1987).

[15]P. Hargraves and R. A. Dunlap, J. Magn. Magn. Mater. **75**,

378 (1988).
[16]M. Miglierini, J. Sitek, L. Macko, M. Mihalik, and A. Zentko, Hyperfine Interact. **60**, 695 (1990).
[17]M. Miglierini, J. Mater. Sci. Lett. **9**, 497 (1990).
[18]M. Miglierini, J. Mater. Sci. **26**, 4255 (1991).
[19]I. Škorvánek, B. Idzikowski, A. Zentko, and E. Mosiniewicz-Szablewska, Phys. Status Solidi A **108**, 747 (1988).
[20]F. P. Schimansky, R. Gerling, and R. Wagner, Mater. Sci. Eng. **97**, 173 (1988).
[21]M. Miglierini and I. Škorvánek, Mater. Sci. Eng. (to be published).
[22]H. Kronmüller, J. Phys. (Paris) Colloq. **41**, C8-618 (1980).
[23]A. Gupta, S. Habibi, S. Lal, and G. Principi, Hyperfine Interact. **55**, 967 (1990).
[24]S. Nasu and F. E. Fujita, Hyperfine Interact. **29**, 1279 (1986).
[25]N. Hayashi, T. Toriyama, I Sakamoto, and K. Hisatake, J. Phys. Condens. Matter **1**, 3849 (1989).
[26]R. A. Dunlap, D. W. Lawther, P. Hargraves, and P. Sinclair, J. Phys. F. **18**, 2479 (1988).
[27]I. Škorvánek and M. Miglierini, J. Magn. Magn. Mater. **96**, 762 (1991).
[28]S. N. Kaul, Phys. Rev. B **22**, 278 (1980).
[29]T. Egami, IEEE Trans. Magn. **MAG-17**, 2600 (1981).
[30]M. Piecuch, G. Marschal, Ph. Mangin, and Chr. Janot, Phys. Status Solidi A **62**, K99 (1980).
[31]G. L. Whittle, S. J. Campbell, and A. M. Stewart, Phys. Status Solidi A **71**, 245 (1982).
[32]R. V. Vadnere, V. Srinivas, A. K. Nigam, G. Rajaram, G. Chandra, S. Prasad, S. N. Shringi, and R. Krishnan, Hyperfine Interact. **42**, 955 (1988).
[33]G. Rajaram, S. Prasad, G. Chandra, S. N. Shringi, and R. Krishnan, Phys. Lett. **98A**, 57 (1983).
[34]C. L. Chien, Phys. Rev. B **19**, 81 (1979).
[35]C. L. Chien and H. S. Chen, J. Appl. Phys. **50**, 1574 (1979).
[36]A. M. Stewart and G. L. Whittle, in *Rapidly Quenched Metals,* edited by S. Steeb and H. Warlimont (North-Holland, Amsterdam, 1985), p. 553.
[37]T. G. Narendra Babu, R. Jagannathan, A. K. Bhatnager, and V. R. V. Ramanan, Hyperfine Interact. **27**, 293 (1986).
[38]V. M. Agranovich and V. V. Kirsanov, in *Physics of Radiation Effects in Crystals,* edited by R. A. Johnson and A. N. Orlov (North-Holland, Amsterdam, 1986), p. 117.